

# Noise-induced intermittency in a superconducting microwave resonator

G. BACHAR<sup>1(a)</sup>, E. SEGEV<sup>1</sup>, O. SHTEMPLUCK<sup>1</sup>, S. W. SHAW<sup>2</sup> and E. BUKS<sup>1</sup>

<sup>1</sup> *Department of Electrical Engineering - Technion, Haifa 32000, Israel*

<sup>2</sup> *Department of Mechanical Engineering, Michigan State University - East Lansing, MI 48824-1226 USA*

received 16 August 2009; accepted in final form 13 December 2009

published online 22 January 2010

PACS 74.40.+k – Fluctuations (noise, chaos, nonequilibrium superconductivity, localization, etc.)

PACS 84.40.Dc – Microwave circuits

PACS 85.25.-j – Superconducting devices

**Abstract** – We experimentally and numerically study a NbN superconducting stripline resonator integrated with a microbridge. We find that the response of the system to monochromatic excitation exhibits intermittency, namely, noise-induced jumping between coexisting steady-state and limit-cycle responses. A theoretical model that assumes piecewise linear dynamics yields partial agreement with the experimental findings.

Copyright © EPLA, 2010

Nonlinear response of superconducting RF devices can be exploited for a variety of applications such as noise squeezing [1], bifurcation amplification [2–4] and resonant readout of qubits [5]. Recently we have reported on an instability found in NbN superconducting stripline resonators in which a short section of the stripline was made relatively narrow, forming thus a microbridge [6,7]. In these experiments a monochromatic pump tone, having a frequency close to one of the resonance frequencies, is injected into the resonator and the reflected power off the resonator is measured. We have discovered that there is a certain zone in the pump frequency - pump amplitude plane, in which the resonator exhibits limit-cycle (LC) response resulting in self-sustained modulation of the reflected power. Moreover, to account for the experimental findings we have proposed a simple piecewise linear model, which attributes the resonator's nonlinear response to thermal instability occurring in the microbridge [8]. In spite of its simplicity, this model yields a rich variety of dynamical effects. In particular, as we show below, it predicts the occurrence of intermittency, namely the coexistence of different LC and steady-state solutions, and noise-induced jumping between them.

In the present paper we study both theoretically and experimentally noise-induced transitions between different metastable responses. We employ a 1D map to identify the possible LC solutions of the system and to find conditions for the occurrence of intermittency.

Experimentally we present measurements showing both, intermittency between an LC and a steady state, and intermittency between different LCs. A comparison between the experimental results and theory yields a partial agreement.

Intermittency is a phenomenon in which a system response remains steady for periods of time (the laminar phase) which are interrupted by irregular spurts of relatively large amplitude dynamics (the turbulent phase). It arises in certain deterministic systems that are near a bifurcation in which a steady response is destabilized or destroyed [9]. This phenomenon also occurs in noisy systems in which the laminar response has a weak point in its local basin of attraction and is randomly bumped across the basin threshold, and then ultimately reinjected back to the laminar state, and the process repeats. This latter type of bursting behavior, which is relevant to the present system, is observed to occur in many other systems, including Rayleigh-Bénard convection [10], acoustic instabilities [11], turbulent boundary layers [12], semiconducting lasers [13], blinking quantum dots [14], sensory neurons [15], cardiac tissues [16], micro- and nanomechanical systems [17–19] and Josephson junctions [20]. The presence and level of noise has a significant effect on all such systems, since perturbations affect the triggering of the system out of the laminar phase [21,22]. The mean duration times of the laminar phase for a certain class of these systems scales in a manner that depends on the bifurcation parameter and the noise level [23,24]. A special feature of the present system is that it exhibits

<sup>(a)</sup>E-mail: gil@tx.technion.ac.il

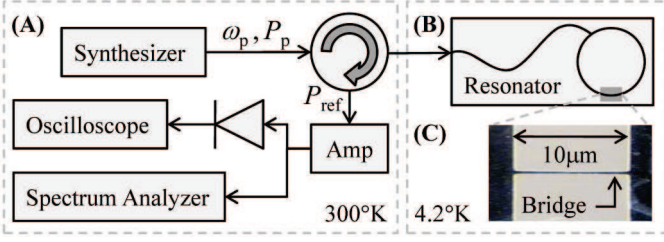


Fig. 1: (A) Measurement setup. (B) Schematic layout of the device. (C) Optical microscope image of the straight shaped microbridge.

a very sharp transition between two types of operating states, namely, normal conducting (NC) and superconducting (SC), which is modeled by equations with discontinuous characteristics. While the deterministic behavior of such nonsmooth systems (at least of low order) is generally well understood, including local and global bifurcations [25], the effects of noise in such systems has not been considered.

The present experiments are performed using the setup depicted in fig. 1(A). The resonator is stimulated with a monochromatic pump tone having an angular frequency  $\omega_p$  and power  $P_p$ . The power reflected off the resonator is amplified at room temperature and measured by using both, a spectrum analyzer in the frequency domain and an oscilloscope, tracking the reflected power envelope, in the time domain. All measurements are carried out while the device is fully immersed in liquid helium. A simplified circuit layout of the device is illustrated in fig. 1(B). The resonator is formed as a stripline ring made of niobium nitride (NbN) deposited on a sapphire wafer [26,27], and having a characteristic impedance of  $50 \Omega$ . A feedline, which is weakly coupled to the resonator, is employed for delivering the input and output signals. A microbridge is monolithically integrated into the structure of the ring [28]. Further design considerations, fabrication details as well as normal modes calculation can be found elsewhere [26].

The dynamics of our system can be captured by two coupled equations of motion, which are hereby briefly described (see ref. [8] for a detailed derivation). Consider a resonator driven by a weakly coupled feedline carrying an incident coherent tone  $b^{\text{in}} = b_0^{\text{in}} e^{-i\omega_p t}$ , where  $b_0^{\text{in}}$  is a constant complex amplitude and  $\omega_p$  is the driving angular frequency. The mode amplitude inside the resonator can be written as  $B e^{-i\omega_p t}$ , where  $B(t)$  is a complex amplitude, which is assumed to vary slowly on a time scale of  $1/\omega_p$ . In this approximation, the equation of motion of  $B$  reads

$$\frac{dB}{dt} = [i(\omega_p - \omega_0) - \gamma] B - i\sqrt{2\gamma_1} b^{\text{in}} + c^{\text{in}}, \quad (1)$$

where  $\omega_0$  is the angular resonance frequency and  $\gamma = \gamma_1 + \gamma_2$ , where  $\gamma_1$  is the coupling coefficient between the resonator and the feedline and  $\gamma_2$  is the damping rate of the mode. The term  $c^{\text{in}}$  represents an input Gaussian

noise, whose time autocorrelation function is given by  $\langle c^{\text{in}}(t) c^{\text{in}*}(t') \rangle = G \omega_0 \delta(t - t')$ , where the constant  $G$  can be expressed in terms of the effective noise temperature  $T_{\text{eff}}$  as  $G = (2\gamma/\omega_0)(k_B T_{\text{eff}}/\hbar\omega_0)$ . Note that in our experiment, in addition to thermal contribution, a phase noise of the signal source also has a significant contribution to the total noise, and consequently the effective temperature of the noise  $T_{\text{eff}}$  can be higher than coolant temperature of 4.2 K and even higher than room temperature. The effective noise temperature  $T_{\text{eff}}$  is determined by numerically fitting to experimental data.

The microbridge heat balance equation reads

$$C \frac{dT}{dt} = 2\hbar\omega_0\gamma_2\alpha |B|^2 - H(T - T_0), \quad (2)$$

where  $T$  is the temperature of the microbridge,  $C$  is the thermal heat capacity,  $\alpha$  is the portion of the heating power applied to the microbridge relative to the total power dissipated in the resonator ( $0 \leq \alpha \leq 1$ ),  $H$  is the heat transfer coefficient, and  $T_0 = 4.2$  K is the temperature of the coolant.

Coupling between eqs. (1) and (2) originates by the dependence of the parameters of the driven mode  $\omega_0$ ,  $\gamma_1$ ,  $\gamma_2$  and  $\alpha$  on the resistance and inductance of the microbridge, which in turn depend on its temperature. We assume the simplest case, where this dependence is a step function that occurs at the critical temperature  $T_c \simeq 10$  K of the superconductor, namely  $\omega_0$ ,  $\gamma_1$ ,  $\gamma_2$  and  $\alpha$  take the values  $\omega_{0s}$ ,  $\gamma_{1s}$ ,  $\gamma_{2s}$  and  $\alpha_s$ , respectively, for the SC phase ( $T < T_c$ ) of the microbridge and  $\omega_{0n}$ ,  $\gamma_{1n}$ ,  $\gamma_{2n}$  and  $\alpha_n$ , respectively, for the NC phase ( $T > T_c$ ). The assumption that the parameters characterizing the resonator have a step function dependence on temperature greatly simplifies the problem at hand since this assumption yields piecewise linear dynamics. In reality, however, the transition has a finite width (see our previous work [26]). To investigate the dependence on the transition width we have substituted the step function dependence by a hyperbolic tangent dependence to model a smooth transition. We have found, however, that the results are almost unchanged provided that the temperature peak to peak amplitude of self-oscillations is much larger than the transition width.

Solutions of steady-state response to a monochromatic excitation are found by seeking stationary solutions to eqs. (1) and (2) for the noiseless case  $c^{\text{in}} = 0$ . The system may have, in general, up to two locally stable steady states, corresponding to the SC and NC phases of the microbridge. The stability of each of these phases depend on the corresponding steady state values  $B_s = i\sqrt{2\gamma_1} b^{\text{in}} / [i(\omega_p - \omega_{0s}) - \gamma_s]$  and  $B_n = i\sqrt{2\gamma_1} b^{\text{in}} / [i(\omega_p - \omega_{0n}) - \gamma_n]$  (see eq. (1)). An SC steady state exists only if  $|B_s|^2 < E_s$ , where  $E_s = H(T_c - T_0)/2\hbar\omega_{0s}\gamma_{2s}\alpha_s$ , whereas a NC steady state exists only if  $|B_n|^2 > E_n$ , where  $E_n = H(T_c - T_0)/2\hbar\omega_{0n}\gamma_{2n}\alpha_n$ . Consequently, four stability zones can be identified in the plane of pump power  $P_p \propto |b_0^{\text{in}}|^2$  - pump frequency  $\omega_p$  (see fig. 2) [8].

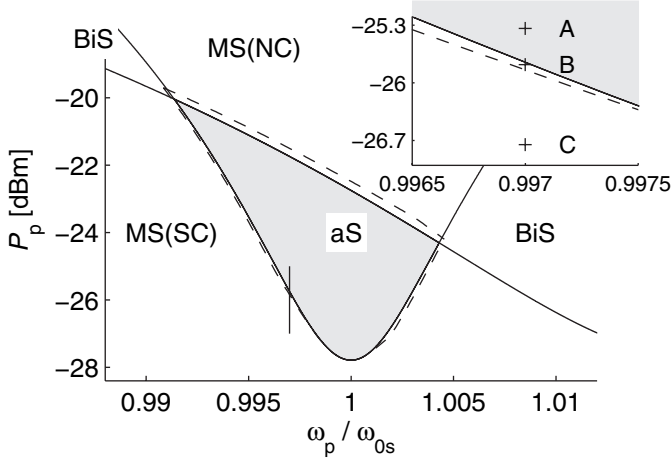


Fig. 2: Stability zones in the  $\omega_p$ - $P_p$  plane: SC monostable (MS(SC)), NC monostable (MS(NC)), bistable (BiS), and astable (aS) (gray colored) zones. The region where a stable LC exists is marked with a dashed line. The inset shows the three operating points (A, B and C) at which the measurements and theoretical analysis shown in figs. 3 and 4 are done. The following parameters were used in the numerical simulation:  $\omega_{0s}/2\pi = 3.49$  GHz,  $\gamma_{1s} = 1.14e - 3\omega_{0s}$ ,  $\gamma_{2s} = 2.74e - 3\omega_{0s}$ ,  $\omega_{0n}/\omega_{0s} = 1.017\omega_{0s}$ ,  $\gamma_{1n} = 1.14 \times 10^{-2}\omega_{0s}$  and  $\gamma_{2n} = 2.74 \times 10^{-2}\omega_{0s}$ ,  $C = 15.4$  fJ/K,  $H/C = 0.211\omega_{0s}$ ,  $T_{\text{eff}} = 700$  K.  $\omega_p = 0.997\omega_{0s}$ ,  $P_p = -25.34$  dBm (A),  $-25.78$  dBm (B),  $-26.75$  dBm (C).

Two are monostable (MS) zones (MS(SC) and MS(NC)), where either the SC or the NC phases is locally stable, respectively. Another is a bistable zone (BiS), where both phases are locally stable. The third is an astable zone (aS), where none of the phases are locally stable.

The task of finding LC solutions of eqs. (1) and (2) can be greatly simplified by exploiting the fact that typically  $\gamma \ll H/C$  in our devices, namely, the dynamics of the mode amplitude  $B$  (eq. (1)) can be considered as slow in comparison with the one of the temperature  $T$  (eq. (2)). In this limit one finds by employing an adiabatic approximation [8] that the temperature  $T$  remains close to the instantaneous value given by  $T_i = T_0 + 2\hbar\omega_0\gamma_2|B|^2/H$  for most of the time except of relatively short time intervals (on the order of  $C/H$ ) right after each switching event between the SC and NC phases. Consequently, as can be seen from the example trajectories shown in fig. 3 (A-1), transitions from SC to NC phase occur near the circle  $|B|^2 = E_s$ , whereas transitions from NC to SC phase occur near the circle  $|B|^2 = E_n$ .

The important features of the system's dynamics can be captured by constructing a 1D map [29]. Consider the case where  $E_n < E_s$  and the amplitude  $B$  lies initially on the circle  $|B|^2 = E_n$ , namely  $B = \sqrt{E_n}e^{2\pi i x}$  where  $x \in [0, 1]$ . Furthermore, assume that initially the system is in the SC phase, namely,  $T < T_c$  and consequently  $B$  is attracted towards the point  $B_s$ . The 1D map  $D(x)$  is obtained by tracking the time evolution of the system for the noiseless

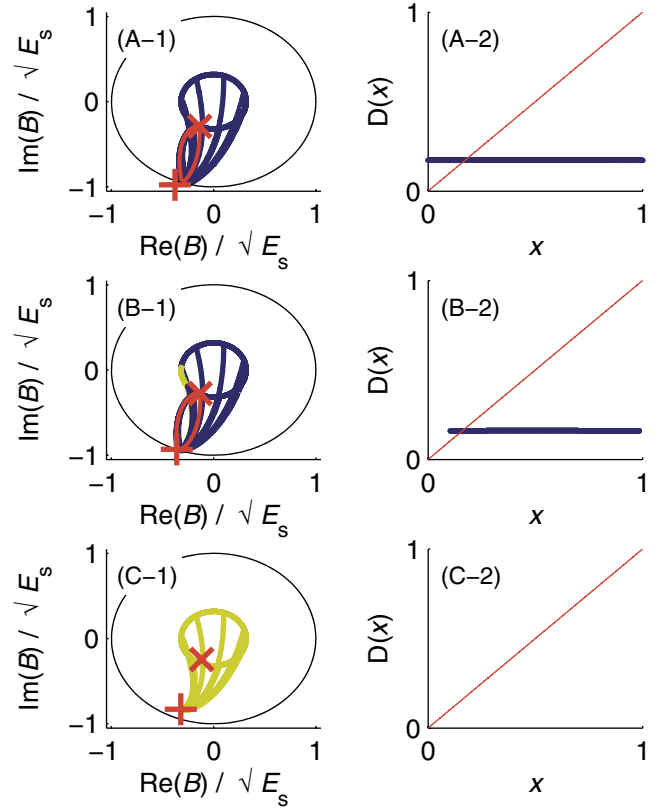


Fig. 3: (Color online) Resonator's dynamics. Subplots A, B and C, correspond to the three operating points A, B and C, respectively, which are marked in the inset of fig. 2. In subplot (A) only an LC is locally stable, in subplot (B) intermittency between an LC and an SC steady state occurs, whereas only an SC steady state is locally stable in subplot (C). In panels (A-1), (B-1) and (C-1), which show the time evolution in the  $B$  plane, a plus sign labels  $B_s$  and a cross sign labels  $B_n$ . These points are shown for reference and correspond to fixed points of the dynamics only when they exist in their respective domains, as defined in the text. Trajectories that return to the inner circle  $|B|^2 = E_n$  are colored in blue (dark gray), and trajectories that end at  $B_s$  are colored in yellow (light gray). Panels (A-2), (B-2) and (C-2) show the corresponding 1D maps.

case ( $c^{\text{in}} = 0$ ) until the next time it returns to the circle  $|B|^2 = E_n$  to a point  $B = \sqrt{E_n}e^{2\pi i D(x)}$  where  $D(x) \in [0, 1]$ . In the adiabatic limit this can be done using eq. (1) only (without explicitly referring to eq. (2)) since switching to the NC phase in this case occurs when the trajectory intersects with the circle  $|B|^2 = E_s$ . Note that in the aS zone of operation all points on the circle  $|B|^2 = E_n$  return back to it after a finite time. However, this is not necessarily the case in the other stability zones. Therefore, we restrict the definition of the 1D map  $D(x)$  only for points on the circle  $|B|^2 = E_n$  that eventually return to it. Other points will have a trajectory that ends at a steady state (NC or SC), and thus their existence will show that one of these states is stable. Those points will not appear in the 1D map.

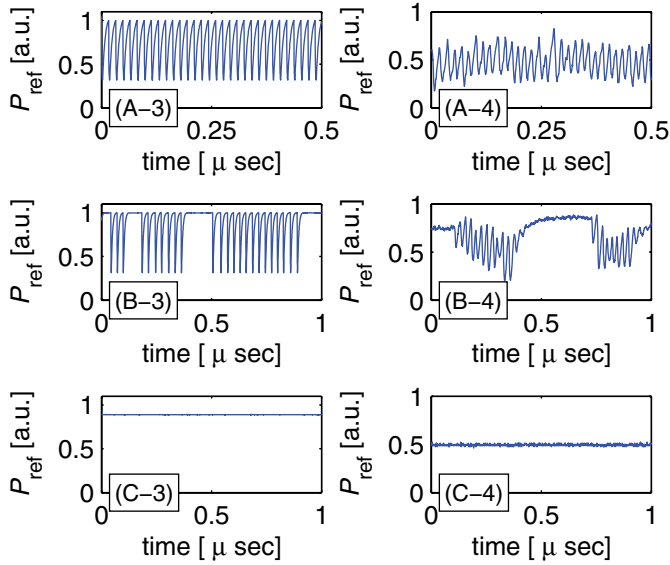


Fig. 4: (Color online) Numerical (panels (A-3), (B-3) and (C-3)) vs. experimental (panels (A-4), (B-4) and (C-4)) time traces for the three operating points A, B and C, respectively.

Any fixed point of the 1D map, namely a point for which  $D(x_0) = x_0$ , represents an LC of the system. The LC is locally stable provided that  $|dD/dx|_{x=x_0} < 1$  [29]. We have scanned the  $\omega_p$ - $P_p$  plane, and using a 1D map for each working point we were able to determine the region where an LC solution exists, which is marked with dashed line in fig. 2. Note that this region extends beyond the aS region due to the possibility of intermittency of a steady-state solution and an LC one.

Figure 3 shows noiseless behavior of the resonator for the three operating points A, B and C, which lie near the border between the aS region and the MS(SC) one, and are marked in the inset of fig. 2. Figure 4 shows a comparison of experimental data and numerical simulation for these operating points. The sample parameters used in the numerical simulations and are listed in the caption of fig. 2, were determined using the same methods detailed in ref. [8].

Subplot (A) shows the behavior at operating point A, which lies inside the aS zone. In panel (A-1) sample trajectories in the  $B$  plane are shown. The resultant 1D map, which is plotted in panel (A-2), has a single fixed point corresponding to a single locally stable LC. The time evolution seen in panel (A-3) was obtained by numerically integrating the coupled stochastic equations of motion (1) and (2). The trace is then compared to experimental data taken from the same working point (panel (A-4)).

At operating point B (see figs. 3 and 4 subplot (B)) coexistence of an LC and an SC steady state occurs. The LC corresponds to the locally stable fixed point of the 1D map seen in panel (B-2). On the other hand, all initial points on the circle  $|B|^2 = E_n$  that never return to it evolve towards the SC steady state  $B_s$ . Numerical time

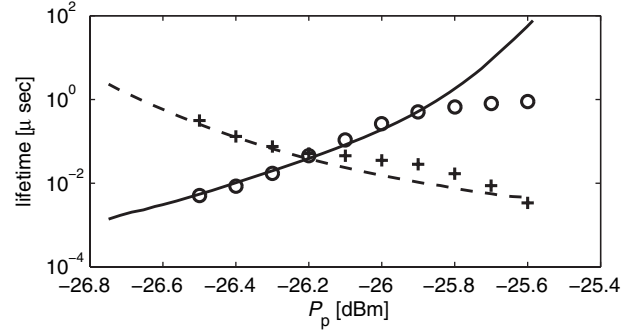


Fig. 5: Experimental data of the lifetime of LC (circles) and steady state (crosses) compared to numerical prediction (solid and dashed lines, respectively). The measurements above  $-28.5$  dBm saturate to  $1 \mu\text{s}$  as this is the maximal mesurement time.

evolution shows noise-induced transitions between the two metastable solutions (panel (B-3)). Experimental data for the same working point exhibits similar behavior (panel (B-4)). At operating point C (see figs. 3 and 4 subplot (C)) the LC has been annihilated by a discontinuity-induced bifurcation [25] and consequently only steady-state response is observed.

The noise-induced transitions, demonstrated in working point B can be understood as follows: In general, each solution (steady state or LC) can be characterized by a basin of attraction in the 3-dimensional phase space of the system (having 3 coordinates  $\text{Re}(B)$ ,  $\text{Im}(B)$  and  $T$ ). A transition between different solutions occurs when the system exits the basin of attraction of an initial solution due to fluctuations induced by external noise.

To further study noise-induced transitions we fixed  $\omega_p$  and vary  $P_p$  starting from MS(SC) zone  $P_p = -26.7$  dBm to the aS zone  $P_p = -25.6$  dBm (see the vertical line in fig. 2), and took relatively long time traces of the reflected power (similar to those seen in figs. 4(A-4), (B-4) and (C-4)). The average lifetime of both LC and SC steady state, namely, the average time the system is in one solution before making a transition to the other one, were determined from these traces. This data, compared to numerical simulation prediction (using the parameters listed in the caption of fig. 2) is shown in fig. 5. While the problem of lifetime calculation of a steady-state solution has been thoroughly studied for the case of smooth systems [30], very little is currently known about lifetime of LC solutions, or lifetime in nonsmooth systems [31]. We hope that our results will motivate further theoretical study of these problems.

In spite of its simplicity, our model, as was demonstrated above, can successfully reproduce many of the experimental observations. However, as we point out below, some of the results were left unaccountable. In another experiment using a similar device we observe intermittency of two different LCs (see fig. 6). Panel (A) shows spectrum analyzer measurement of the reflected power as a



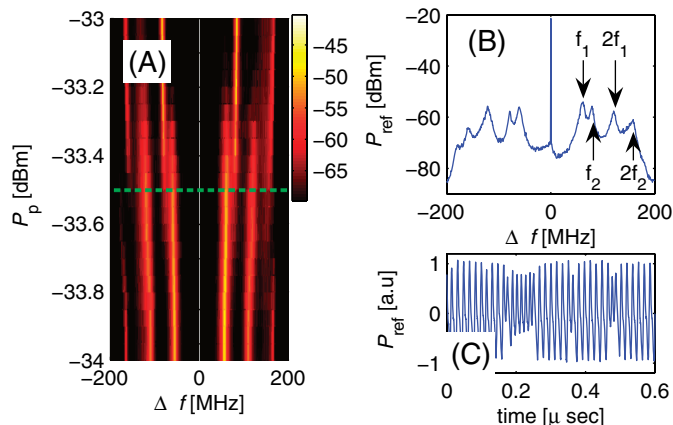


Fig. 6: (Color online) Experimental demonstration of intermittency between two LCs. Panel (A) shows a spectrum analyzer measurement of the reflected power  $P_{\text{ref}}$  as a function of the offset frequency  $\Delta f$  (with respect to the pump frequency  $\omega_p/2\pi = 6.61$  GHz) and the pump power  $P_p$ . Panel (B) shows a cross-section of panel (A) obtained at the value of  $P_p = -33.5$  dBm, which is indicated by a dashed line. The frequencies  $f_1$  and  $f_2$  of the two LCs are indicated by arrows. Panel (C) shows a time trace of the reflected power taken at the same value of  $P_p$ .

function of the pump power  $P_p$ . Two distinct LCs having frequencies  $f_1 \simeq 60$  MHz and  $f_2 \simeq 80$  MHz are observed. For low pump powers ( $P_p < -33.5$  dBm) only an LC at frequency  $f_1$  is visible. In the range  $-33.55$  dBm  $< P_p < -33.35$  dBm both LCs are seen, whereas for high pump power  $P_p > -33.5$  dBm only an LC at frequency  $f_2$  is seen. Panel (B), which shows a cross-section of panel (A) at pump power of  $P_p = -33.5$  dBm (indicated by a dashed line in panel (A)), demonstrates the behavior in the intermediate region, where both LCs are observed. Panel (C) shows the transitions in the time domain corresponding to the same pump power  $P_p = -33.5$  dBm.

In general, intermittency of two (or more) different LCs can be theoretically reproduced using our simple model. However, we were unable to numerically obtain this behavior without significantly varying some of the system's experimental parameters. This discrepancy between experimental and theoretical results suggest that a further theoretical study is needed in order to develop a more realistic description of the system. Such description would have to exclude some of the simplifying assumptions that were made to derive our model.

\*\*\*

We thank M. CROSS, M. DYKMAN, O. GOTTLIEB and R. LIFSHITZ for valuable discussions and helpful comments. This work was supported by the Israel Science Foundation under grant 1380021, the Deborah Foundation, the Poznanski Foundation, Russel Berrie Nanotechnology Institute, and MAFAT.

## REFERENCES

- [1] MOVSHOVICH R., YURKE B., KAMINSKY P. G., SMITH A. D., SILVER A. H., SIMON R. W. and SCHNEIDER M. V., *Phys. Rev. Lett.*, **65** (1990) 1419.
- [2] SIDDIQI I., VIJAY R., PIERRE F., WILSON C. M., METCALFE M., RIGETTI C., FRUNZIO L. and DEVORET M. H., *Phys. Rev. Lett.*, **93** (2004) 207002.
- [3] CASTELLANOS-BELTRAN M. A. and LEHNERT K. W., *Appl. Phys. Lett.*, **91** (2007) 83509.
- [4] THOLEN E. A., ERGUL A., DOHERTY E. M., WEBER F. M., GREGIS F. and HAVILAND D. B., *Appl. Phys. Lett.*, **90** (2007) 253509.
- [5] LEE J. C., OLIVER W. D., BERGGREN K. K. and ORLANDO T. P., *Phys. Rev. B*, **75** (2007) 144505, <http://prb.aps.org/abstract/PRB/v75/i14/e144505>.
- [6] SEGEV E., ABDO B., SHTEMPLUCK O. and BUKS E., *Phys. Lett. A*, **366** (2007) 160.
- [7] SEGEV E., ABDO B., SHTEMPLUCK O. and BUKS E., *Euro. Phys. Lett.*, **78** (2007) 57002.
- [8] SEGEV E., ABDO B., SHTEMPLUCK O. and BUKS E., *J. Phys.: Condens. Matter*, **19** (2007) 96206.
- [9] BERGE P., POMEAU Y. and VIDAL C., *Order Within Chaos* (Wiley, New York) 1984.
- [10] ECKE R. and HAUCKE H., *J. Stat. Phys.*, **54** (1989) 1153.
- [11] FRANCK C., KLINGER T. and PIEL A., *Phys. Lett. A*, **259** (1999) 152.
- [12] STONE E. and HOLMES P., *Physica D*, **37** (1989) 20.
- [13] PEDACI F., GIUDICI M., TREDICCE J. R. and GIACOMELLI G., *Phys. Rev. E*, **71** (2005) 36125.
- [14] KUNO M., FROMM D. P., HAMANN H. F., GALLAGHER A. and NESBITT D. J., *J. Chem. Phys.*, **112** (2000) 3117.
- [15] LONGTIN A., BULSARA A. and MOSS F., *Phys. Rev. Lett.*, **67** (1991) 656.
- [16] CHIALVO and JALIFE J., *Cardiac Electrophysiology: From Cell to Bedside* (Saunders) 1990, pp. 201–214, Chapt. 24.
- [17] CHAN H. B. and STAMBAUGH C., *Phys. Rev. B*, **73** (2006) 224301.
- [18] ALDRIDGE J. S. and CLELAND A. N., *Phys. Rev. Lett.*, **94** (2005) 156403.
- [19] STAMBAUGH C. and CHAN H. B., *Phys. Rev. B*, **73** (2006) 172302, <http://prb.aps.org/abstract/PRB/v73/i17/e172302>.
- [20] SIDDIQI I., VIJAY R., PIERRE F., WILSON C. M., FRUNZIO L., METCALFE M., RIGETTI C., SCHOELKOPF R. J., DEVORET M. H., VION D. and ESTEVE D., *Phys. Rev. Lett.*, **94** (2005) 027005.
- [21] ECKMANN J., THOMAS L. and WITWER P., *J. Phys. A: Math Gen.*, **14** (1981) 3153.
- [22] HAUCKE H., ECKE R. E., MAENO Y. and WHEATLEY J. C., *Phys. Rev. Lett.*, **53** (1984) 2090.
- [23] SOMMERER J., OTT E. and GREBOGI C., *Phys. Rev. A*, **43** (1991) 1754.
- [24] SOMMERER J. C., DITTO W. L., GREBOGI C., OTT E. and SPANO M. L., *Phys. Rev. Lett.*, **66** (1991) 1947.
- [25] BERNARDO M. D., BUDD C., CHAMPNEYS A. and KOWALCZYK P., *Piecewise-Smooth Dynamical Systems: Theory and Applications*, *Appl. Math. Sci. Ser.*, Vol. **163** (Springer-Verlag) 2007.

- [26] SEGEV E., ABDO B., SHTEMPLUCK O. and BUKS E., *IEEE Trans. Appl. Supercond.*, **16** (2006) 1943.
- [27] CHANG K., MARTIN S., WANG F. and KLEIN J. L., *IEEE Trans. Microwave Theory Tech.*, **35** (1987) 1288.
- [28] SAEEDKIA D., MAJEDI A. H., SAFAVI-NAEINI S. and MANSOUR R. R., *IEEE Microwave Wirel. Compon. Lett.*, **15** (2005) 510.
- [29] STROGATZ S., *Nonlinear Dynamics and Chaos: With Applications to Physics, Biology, Chemistry and Engineering* (Perseus Books Group) 2000.
- [30] HANGGI P., TALKNER P. and BORKOVEC M., *Rev. Mod. Phys.*, **62** (1990) 251.
- [31] SEGEV E., ABDO B., SHTEMPLUCK O. and BUKS E., *Phys. Rev. B*, **77** (2008) 12501.